

¹ **Short Large-Amplitude Magnetic Structures**
² **(SLAMS) at Venus**

G.A. Collinson^{1†}, L.B. Wilson^{1†}, D.G. Sibeck¹, N. Shane^{2,3}, T.L. Zhang⁴,
T.E. Moore¹, A.J. Coates², and S. Barabash⁵

³ † - *Authors contributed equally to this study.*

¹Heliophysics Science Division, NASA
Goddard Spaceflight Center, Greenbelt,
Maryland, USA.

²Mullard Space Science Laboratory,
University College London, Holmbury St.
Mary, Surrey, UK.

³The Centre for Planetary Sciences at
UCL/Birkbeck, London, UK

⁴Austrian Academy of Sciences, Space
Research Institute, Graz, Austria

⁵Swedish Institute of Space Physics,
Kiruna, Sweden

Abstract.

5 We present the first observation of magnetic fluctuations consistent with
6 Short Large-Amplitude Magnetic Structures (SLAMS) in the foreshock of
7 the planet Venus. Three monolithic magnetic field spikes were observed by
8 the *Venus Express* on the 11th of April 2009. The structures were $\sim 1.5\text{--}11s$
9 in duration, had magnetic compression ratios between $\sim 3\text{--}6$, and exhibited
10 elliptical polarization. These characteristics are consistent with the SLAMS
11 observed at Earth, Jupiter, and Comet Giacobini-Zinner, and thus we hy-
12 pothesize that it is possible SLAMS may be found at any celestial body with
13 a foreshock.

14

1. Introduction

15 The foreshock is the region of space upstream from a celestial body which is magnet-
16 ically connected to the bow shock [*Eastwood et al.*, 2005]. It is pervaded by a field of
17 ULF waves [*Fairfield*, 1969; *Scarf et al.*, 1970] which are thought to be driven by field-
18 aligned ion beams reflected at the bow shock [*Tsurutani and Rodriguez*, 1981; *Hoppe and*
19 *Russell*, 1983], or produced locally [*Hellinger and Mangeney*, 1999; *Mazelle et al.*, 2003;
20 *Meziane et al.*, 2004]. ULF waves have been observed at many planets including Venus
21 [*Hoppe and Russell*, 1981], Jupiter [*Tsurutani et al.*, 1993b], and at interplanetary shocks
22 [*Tsurutani et al.*, 1983]. The waves attempt to propagate upstream, but are convected
23 back toward the bow shock by the solar wind. As they convect deeper into the foreshock,
24 they enter regions of higher diffuse ion density. These ions alter the index of refraction
25 for the medium causing transverse modes to become compressive, and thus the waves can
26 steepen [e.g. *Wilson et al.*, 2009; *Tsubouchi and Lembège*, 2004; *Tsurutani et al.*, 1987,
27 and references therein]. They become more oblique and compressional the deeper they go.

28
29 One of the possible resulting foreshock phenomena are Short Large-Amplitude Magnetic
30 Structures (SLAMS), pulsations believed to steepen out of the background ULF wave field
31 due to the interaction with diffuse ions [e.g. *Scholer et al.*, 2003; *Dubouloz and Scholer*,
32 1995]. As the waves convected back toward the bow shock, the different wave fronts (i.e.
33 wave crests and troughs) cause a differential slowing of the incident solar wind flow which
34 leads to the refraction of the waves. As the amplitude of the SLAMS increases, their
35 phase speed also increases. *Dubouloz and Scholer* [1995] found that SLAMS are left hand

36 polarized in the plasma frame, that both upstream and downstream edges steepen, and
37 that some pulsations appear to nearly stand against the incident flow. SLAMS are dis-
38 tributed over a transition region of 2-3 R_E , with individual scale sizes of $\sim 700 \rightarrow 1000 km$,
39 or $\sim 10 \rightarrow 15$ ion inertial lengths.

40

41 SLAMS are elliptically polarized and compressive characterized by brief (5 – 20s) mono-
42 lithic spikes in magnetic field magnitude ($|B|$), with compression ratio ($\delta B/B_0$) between 2
43 to 5 times the background field [*Schwartz, 1991; Tsurutani et al., 1993a; Schwartz et al.,*
44 *1992; Dubouloz and Scholer, 1993*]. They are commonly observed in the quasi-parallel
45 (i.e. where the angle between the magnetic field vector and the normal to the bow shock,
46 $\theta_{Bn} < 45^\circ$) foreshock when and where the Interplanetary Magnetic Field (IMF) lies quasi-
47 parallel to the bow shock normal [*Schwartz, 1991*].

48

49 As SLAMS convect Earthwards, their phase speed increases as their amplitude increases
50 [*Omidi and Winske, 1990*]. Thus their motion relative to the planet decreases, and they
51 coalesce together to form the complex three-dimensional patchwork of the quasi-parallel
52 shock [*Schwartz and Burgess, 1991; Lucek et al., 2008*] (although not all observations of
53 quasi-parallel shocks are thought to obey this paradigm [*Burgess, 1995*]). Thus, under-
54 standing SLAMS is crucial to understanding how the Earth's shock forms under certain
55 IMF conditions.

56

57 The first extra-terrestrial observation of “*steepened magnetosonic waves*” consistent with
58 SLAMS was made by *Tsurutani et al. [1990]* at Comet Giacobini-Zinner. The pulses ex-

59 hibited compression ratios ($\delta B/B_0$) of 2.3 to 7.0, had full-width half-maximum durations
60 from 12 to 72s, comparable to the H₂O group ion gyroperiod (67s in a 15nT field), and
61 were circularly polarized with right-hand rotation in the spacecraft frame. Later *Tsuru-*
62 *tani et al.* [1993a, b] reported the discovery of large-amplitude magnetic pulses upstream
63 of the Jovian bow shock by *Ulysses*. The magnetic pulses they reported were similar to
64 SLAMS in that they were planar elliptically polarized structures, although their peak am-
65 plitudes were lower ($0.5 \rightarrow 2 |B_0|$) than typically observed at the Earth, and the duration
66 of the pulses was much longer (~ 1 minute).

67
68 In this paper we present the first observations of magnetic pulsations consistent with
69 SLAMS in the Cytherean foreshock by the ESA *Venus Express* [*Svedhem et al.*, 2007]
70 magnetometer [*Zhang et al.*, 2006]. We also present supplementary data from the Anal-
71 yser of Space Plasmas and Energetic Atoms (ASPERA) Electron Spectrometer (ELS)
72 [*Barabash et al.*, 2007], although direct measurement of the plasma properties of the
73 SLAMS were not possible due to limits in the temporal resolution, and low sensitivity
74 [*Collinson et al.*, 2009] owing to a reduced geometric factor [*Collinson et al.*, 2012b] of
75 ASPERA-ELS.

76
77 Our paper is outlined as follows: In section 2 we present a global overview of the Cytherean
78 foreshock encounter by the *Venus Express* on the 11th of April 2009; In section 3.1 we
79 present observations of the ~ 2 minute period in which three SLAMS were observed; In
80 section 3.3 we present an example of our analysis of the magnetic field data from an
81 ~ 11 second period containing three SLAMS; and in section 4 we summarize our find-

82 ings and compare the Cytherean SLAMS with their Terrestrial, Jovian, and Cometary
83 counterparts.

2. Overview of Cytherean upstream conditions on the 11th of April 2009

84 In this section we present data from the ~ 12 minute period that begins in the distant
85 foreshock region where magnetic fluctuations consistent with SLAMS were observed, con-
86 tinues through the three bow shock crossings observed that day, and ends when the *Venus*
87 *Express* goes into the magnetosheath for the third and final time. This global overview
88 puts our later description of Cytherean SLAMS into context.

2.1. Review of Cytherean induced magnetosphere

89 Although Venus has no intrinsic magnetic field [*Smith et al.*, 1965], its conductive iono-
90 sphere creates an impassable barrier to the IMF [*Zhang et al.*, 1991]. Magnetic field lines
91 frozen into the solar wind flow collide with the planetary ionosphere and pile up on the
92 day-side, resulting in the generation of an induced magnetosphere [*Zhang et al.*, 2008].
93 This induced magnetic field is an obstacle to the supersonic solar wind and thus a su-
94 personic bow shock is generated [*Ness et al.*, 1974; *Russell et al.*, 1979]. The stand-off
95 distance of the Cytherean bow shock is much less than that at the Earth, with a closest
96 altitude of ~ 1.5 Venus Radii (R_V) [*Slavin et al.*, 1980], as compared to $\approx 15 R_E$ [*Fairfield*,
97 1971]. The *Venus Express* is in an elliptical quasi-polar orbit with a period of ~ 24 hours,
98 with an apogee over the south pole of $\approx 12 R_V$ [*Titov et al.*, 2006] and perigee inside the
99 ionosphere over the north pole of $\approx 1.04 R_V$.

2.2. Map of Orbit 1086

Figure 1 shows a map of the relevant orbit (1086) on the 11th of April 2009. Panels A, B, and C show the orbital encounter in Venus Solar Orbital (VSO) coordinates, where x points towards the sun, y points back along the orbital path of the planet, and z points out of the plane of the ecliptic completing the right-hand set. Panel D shows the course of the *Venus Express* in cylindrical coordinates, where the x-axis points towards the sun, and the y-axis represents the radial distance from the planet ($R = \sqrt{(y^2 + z^2)}$). This 2D cylindrical projection allows us to plot the positions of the observed bow shock crossings and SLAMS in relation to the idealised bow shock (black line) of *Slavin et al.* [1980]. The blue line represents the path of the *Venus Express*, the pink circles denote the locations of observed bow shock crossings, the yellow stars denote the location where SLAMS were observed, and the light blue line running parallel to the orbit for a distance between $\sim 2.5R_V \rightarrow 1.9R_V$ shows the part of the orbit from which we present data in this section.

As can be seen from Figure 1, *Venus Express* was approaching the planet along the flanks, from a latitude of $\sim 78^\circ$. The position of the Cytherean bow shock is known to be highly variable [*Slavin et al.*, 1980; *Russell et al.*, 1988; *Martinecz et al.*, 2008], and three distinct bow shock crossings were observed on the 11th of April 2009. The furthest crossing was significantly further away from the planet than expected from an idealized hyperbolic model ($2.3R_V$ vs. $1.8R_V$).

2.3. Magnetometer and Electron Spectrometer observations

Figure 2 shows magnetometer and ASPERA-ELS measurements from between 02:42:30 and 02:54:30 (The period of the orbit highlighted by the light blue line in Figure 1).

121 Panel A presents a color-coded timeline showing which of the three regions of space (solar
122 wind, foreshock, magnetosheath) the spacecraft was occupying at any given time. The
123 three bow shock crossings are highlighted with pink circles and vertical dotted lines that
124 have been extended throughout the Figure. The magnetic pulsations which we examine
125 in detail are denoted by yellow stars. The light blue track (in Panel A) running parallel
126 to the timeline from 02:43:00 to 02:45:10 highlights the period of the main event where
127 these magnetic pulsations were observed, and will be covered in more detail in Figure 3
128 and accompanying Section 3.1.

129
130 Panels B through E present the four magnetic field components ($|B|, B_x, B_y, B_z$) in VSO
131 coordinates, respectively. The black line is the full 32 samples per second resolution data
132 and the red line is the same data set averaged at $\frac{1}{4}$ samples per second so that trends can
133 be more easily identified. Panel F shows a plot of the shock normal angle, θ_{Bn} , between
134 an extension of the local magnetic field vector to a model bow shock drawn according
135 to *Slavin et al.* [1980]. Periods when there is no data in panel F indicate when there
136 was no connection between the magnetic field and the model bow shock. Panel G shows
137 an electron spectrogram of the plasma observed by ASPERA-ELS. We have over-plotted
138 $|B|$ (y-axis is arbitrary) to highlight trends between magnetic field magnitude and the
139 electron flux.

140
141 There were three encounters with the magnetosheath (marked in pink on the timeline) and
142 associated bow shock crossings (pink circles). The clearest and best example is the final
143 (right most in Figure 2) bow shock crossing at $\sim 02:53:45$, after which the magnetosheath

144 is clearly visible in panel G by an increase in $|B|$, and an increase in flux of electrons
145 over a broad range of energies, consistent with heating at the bow shock [*Pérez-de-Tejada*
146 *et al.*, 2011]. The two other transitions into the sheath at $\sim 02:45:00$ and $\sim 02:52:30$ were
147 brief, but are evident by the change the orientation of the magnetic field, an increase in
148 $|B|$, and an increase in electron flux consistent with that of the final bow shock crossing.
149 Thus the magnetic pulsations of interest (marked by yellow stars on the timeline, although
150 not yet visible at this scale) were observed shortly before a distant bow shock crossing at
151 $\sim 02:45:00$.

152

153 The period preceding the earliest transition into the sheath from $\sim 02:42:30$ until $\sim 02:45:00$
154 is much more turbulent than the solar wind. There was magnetic connectivity to the bow
155 shock, with (θ_{Bn}) initially near $\sim 60^\circ$, and then fluctuating due to magnetic turbulence.
156 It is very important to recall that these angles are based on an idealised nominal bow
157 shock, and the distant bow shock crossing was $\sim 0.5R_V$ further away than predicted by
158 this model (see Figure 1). Given that this most distant magnetosheath crossing was very
159 brief (6.4s), and that it occurred so far from the nominal bow shock, this suggests that
160 this brief shift in the position of the bow shock was due a reaction to some unknown
161 external solar wind stimuli.

162

163 One possible explanation for this outward shift is a Hot Flow Anomaly (HFA) [*Collinson*
164 *et al.*, 2012b]. HFAs are features that form in close proximity to the bow shock at the
165 intersection of certain interplanetary discontinuities with the bow shock. The brief reduc-
166 tions in pressure associated with HFAs can enable both bow shock and magnetopause to

167 move outward far beyond their mean positions [*Sibeck et al.*, 1999]. HFAs exhibit greatly
 168 heated populations of ions and electrons, as well as highly deflected flows. Consistent with
 169 this interpretation, our event exhibited electron signatures consistent with heating, and a
 170 rotation in the magnetic field. In the absence of high time resolution ion measurements,
 171 we cannot comment on any concomitant flow deflections or ion heating. Regardless of the
 172 presence or absence of an HFA, the turbulent magnetic field, magnetic connection to the
 173 bow shock, and shock-like crossing at $\sim 02:45:00$ suggest that the *Venus Express* was in
 174 the foreshock, the region where SLAMS are expected at Earth. We will now take a closer
 175 look at the period covered by the light blue parallel track on the timeline (Panel A.) of
 176 Figure 2.

3. SLAMS at Venus

3.1. Overview of distant foreshock crossing containing SLAMS

177 Figure 3 shows the period when we observed the three magnetic fluctuations which we
 178 identify as SLAMS. We have highlighted three such fluctuations using a yellow bar and
 179 star on the timeline (Panel A) because they also exhibit a brief spike in $|B|$. The periods
 180 when the spacecraft was in the foreshock are marked by a purple bar on the timeline,
 181 and the brief $\sim 6s$ Magnetosheath crossing is marked in pink with associated bow shock
 182 crossings marked by pink circles.

3.2. Observed properties of Cytherean SLAMS

183 The most obvious feature of the three magnetic pulsations highlighted in Figure 3 is the
 184 brief monolithic spikes in $|B|$ at $\sim 02:43:51$, $\sim 44:44$, and $\sim 44:58$. The average compres-
 185 sion ratio was ~ 4 times the background field. The pulsations had durations between

186 $\sim 1.5 \rightarrow 11$ seconds. Additionally, the $(\delta B/B_0)$ of the leading edge of each increases from
 187 $\sim 3 \Rightarrow 6$, as Venus Express approaches the bow shock (or vice-versa). These magnetic
 188 compression ratios are greater than 2, consistent with observations of SLAMS at the Earth
 189 [*Mann et al.*, 1994]. The compression ratios of the two later pulsations was greater than
 190 the maximum factor of four for simple compression [*Gurnett and Bhattacharjee*, 2005],
 191 which is also consistent with observations of SLAMS [*Schwartz et al.*, 1992]. During the
 192 pulsations, the magnetic fields rotate from a quasi-parallel orientation to a locally quasi-
 193 perpendicular orientation, consistent with observations of SLAMS by *Mann et al.* [1994].
 194 At and near the time of the pulsations there are intervals of nearly quasi-parallel bow shock
 195 configurations, although the degree of turbulence is so great that there also disconnections.
 196 As a whole, during the time of the events, we believe this to be a quasi-parallel bow shock.

197

3.3. Minimum variance analysis of Cytherean SLAMS

198 We performed minimum variance analysis (MVA) on subintervals of the time series
 199 using multiple frequency filters to determine the propagation characteristics of the wave.
 200 For more details about this technique, see *Wilson et al.* [2009]. This process was per-
 201 formed on the steepened leading (upstream) edge of the magnetic pulsations. Figure 4
 202 shows magnetometer data from the eleven second period (02:43:50 to 02:44:01) showing
 203 an example of a Short Large-Amplitude Magnetic Structure (SLAMS) at Venus. Panels
 204 A to D show the data in VSO coordinates, where the black line is 32 samples per second
 205 resolution, and the red line is the appropriate subinterval of this data with a $0.2 - 1Hz$
 206 filter applied. Panels E and F of Figure 4 show hodograms of this filtered subinterval
 207 of magnetic field data. Panel E is in VSO co-ordinates, and Panel F is the same data

208 after MVA. All three of the magnetic structures analyzed were left-hand polarized in
 209 the minimum variance direction. However, with only single spacecraft magnetic field ob-
 210 servations, we cannot define the correct sign of this vector [*Khrabrov and Sonnerup, 1998*].

211
 212 The magnetic field was rotated into field-aligned co-ordinates (not shown) to investigate
 213 the polarization of the fluctuations with respect to the quasi-static magnetic field. The
 214 first structure was highly complex. The leading edge spike (as shown in Figure 4) was
 215 both right and left-hand polarized, whereas the trailing edge of the larger structure was
 216 left-hand polarized in the spacecraft frame. The second (far shorter) structure was left-
 217 hand polarized in the spacecraft frame, and the third structure exhibited both left and
 218 right handed components. These results are consistent with simulations [e.g. *Dubouloz*
 219 *and Scholer, 1995*] and previous observations [e.g. *Schwartz et al., 1992; Mann et al., 1994*]
 220 who found that pulsations showed left-hand and right-hand polarization in the simulation
 221 (i.e. spacecraft) frame, with left-hand polarization in the plasma frame. However, it is not
 222 possible to determine the wave polarization in the spacecraft frame using only magnetic
 223 field observations with a single spacecraft.

224
 225 Panel F shows that the leading (upstream) edge of the structure was elliptically po-
 226 larized, consistent with previous observations [*Schwartz et al., 1992; Tsurutani et al.,*
 227 *1993a; Dubouloz and Scholer, 1993*]. Note that previous studies have referred to this
 228 edge as the “trailing” edge [e.g. *Schwartz et al., 1992*]. The eigenvalues of the MVA were
 229 $(\lambda_{mid}/\lambda_{min}) = 101$, and $(\lambda_{max}/\lambda_{min}) = 1.6$, which shows we have a nearly circularly polar-
 230 ized wave. Our MVA analysis showed an average $\theta_{\hat{\mathbf{k}} \cdot \langle \hat{\mathbf{b}} \rangle} \approx \underline{61.7^\circ}$, consistent with previous

231 observations in the terrestrial foreshock [e.g. *Mann et al.*, 1994], and upstream of Comet
 232 Giacobini-Zinner [*Tsurutani et al.*, 1990].

4. Summary and Discussion

233 In this paper we have reported the first observation of Cytherean Short Large-Amplitude
 234 Magnetic Structures (SLAMS) by the *Venus Express* Magnetometer. SLAMS are common
 235 features of the Earth's foreshock, and can be part of the 3D patchwork of magnetic struc-
 236 tures that compose the quasi-parallel bow shock. We believe these magnetic pulsations
 237 to be SLAMS because they share the following properties with their terrestrial equivalents:

238
 239 1. They were observed on interplanetary magnetic field lines connected to the bow
 240 shock, i.e. the foreshock, the region where SLAMS are observed at Earth.

241 2. We observed large-amplitude monolithic spikes in $|B|$ that have compression ratios
 242 greater than a factor of 2 above the background field, ($(\delta B/B_0)$ between $\sim 3 \Rightarrow 6$), with
 243 an average of ~ 4 , consistent with previous observations [e.g. *Schwartz et al.*, 1992; *Mann*
 244 *et al.*, 1994].

245 3. On the whole, the pulsations had higher compression ratios than can be explained
 246 by simple compression, consistent with previous observations [*Schwartz et al.*, 1992].

247 4. They exhibit left-hand elliptical polarization in the spacecraft frame, consistent with
 248 previous observations [*Lucek et al.*, 2004, 2008].

249 5. MVA analysis of one example revealed that it propagated obliquely to the ambient
 250 field with $\theta_{\hat{\mathbf{k}}_s, \langle \hat{\mathbf{b}} \rangle} \approx 61.7^\circ$, consistent with SLAMS [*Mann et al.*, 1994].

251

252 Our findings are consistent with *Tsurutani et al.* [1990], who reported solitary circularly
 253 polarized magnetic pulses at comet Giacobini-Zinner, with typical peak-to-background
 254 compression ratios of ~ 4 , with $\theta_{\mathbf{k} \cdot \langle \hat{\mathbf{b}} \rangle}$ between 55° to 75° . The durations of the Cytherean
 255 SLAMS were consistent with the $\sim 10s$ typically reported at the Earth [*Schwartz, 1991*],
 256 and shorter than the $\sim 60s$ structures observed at Jupiter and $12s \Rightarrow 72s$ at the Comet
 257 (which *Tsurutani et al.* [1990] reported was comparable to the local H_2O group gyroperiod
 258 of $67s$ in a $15nT$ field). The duration of the monolithic peaks was $\sim 1.5s \Rightarrow 11s$, similar
 259 to the local proton gyroperiod of $9.4s$ in a $7nT$ field.

260
 261 Our calculation of $\theta_{\mathbf{k} \cdot \langle \hat{\mathbf{b}} \rangle} \approx 61.7^\circ$ is consistent with SLAMS acting like a local quasi
 262 perpendicular shock, consistent with previous interpretations [*Mann et al., 1994*]. Com-
 263 pressional waves like this perturb the medium, increasing both $|B|$ and plasma density
 264 which are in phase with one another [*Hellinger and Mangeney, 1999*]. However, it is not
 265 possible for us to compare any plasma perturbations with those known to occur at ter-
 266 restrial SLAMS [*Giacalone et al., 1993; Behlke et al., 2003; Dubouloz and Scholer, 1993*]
 267 due to the limitations of ASPERA.

268
 269 Though only three SLAMS were observed, the short period of the compressive leading
 270 edges ($0.4s \Rightarrow 0.7s$) means that they are only clearly visible in the full 32 sample per
 271 second resolution data, and are therefore not evident in browse plots. The three SLAMS
 272 presented here were discovered by chance during a survey of Cytherean Hot Flow Anoma-
 273 lies [*Collinson et al., 2012a*], and further study is needed to determine if SLAMS are a

274 common feature of the Cytherean foreshock, as they are at Earth.

275

276 **Acknowledgments.** This work was supported by an appointment to the NASA Post-
277 doctoral Program at NASA Goddard Spaceflight Center, administered by Oak Ridge
278 Associated Universities through a contract with NASA.

References

- 279 Barabash, S., et al., The Analyser of Space Plasmas and Energetic Atoms (ASPERA-4)
280 for the Venus Express mission, *Planet. Space. Sci.*, *55*, 1772–1792, 2007.
- 281 Behlke, R., M. André, S. C. Buchert, A. Vaivads, A. I. Eriksson, E. A. Lucek, and
282 A. Balogh, Multi-point electric field measurements of Short Large-Amplitude Magnetic
283 Structures (SLAMS) at the Earth’s quasi-parallel bow shock, *Geophys. Res. Lett.*, *30*(4),
284 040,000–1, 2003.
- 285 Burgess, D., Foreshock-shock interaction at collisionless quasi-parallel shocks, *Advances*
286 *in Space Research*, *15*, 159–169, 1995.
- 287 Collinson, G. A., D. O. Kataria, A. J. Coates, S. M. E. Tsang, C. S. Arridge, G. R.
288 Lewis, R. A. Frahm, J. D. Winningham, and S. Barabash, Electron optical study of the
289 Venus Express ASPERA-4 Electron Spectrometer (ELS) top-hat electrostatic analyser,
290 *Measurement Science and Technology*, *20*(5), 055,204–+, 2009.
- 291 Collinson, G. A., et al., The geometric factor of electrostatic plasma analyzers: A case
292 study from the Fast Plasma Investigation for the Magnetospheric Multiscale mission,
293 *Review of Scientific Instruments*, *83*(3), 033,303, 2012a.
- 294 Collinson, G. A., et al., Hot Flow Anomalies at Venus, *Journal of Geophysical Research*

- 295 (*Space Physics*), 117(A16), A04204, 2012b.
- 296 Dubouloz, N., and M. Scholer, On the origin of short large-amplitude magnetic structures
297 upstream of quasi-parallel collisionless shocks, *Geophys. Res. Lett.*, 20, 547–550, 1993.
- 298 Dubouloz, N., and M. Scholer, Two-dimensional simulations of magnetic pulsations up-
299 stream of the Earth’s bow shock, *J. Geophys. Res.*, 100, 9461–9474, 1995.
- 300 Eastwood, J. P., et al., Observations of multiple X-line structure in the Earth’s mag-
301 netotail current sheet: A Cluster case study, *Geophys. Res. Lett.*, 32, 11,105, doi:
302 10.1029/2005GL022509, 2005.
- 303 Fairfield, D. H., Bow shock associated waves observed in the far upstream interplanetary
304 medium., *J. Geophys. Res.*, 74, 3541–3553, 1969.
- 305 Fairfield, D. H., Average and unusual locations for the earth’s magnetopause and bow
306 shock., *J. Geophys. Res.*, 76, 6700–6716, 1971.
- 307 Giacalone, J., S. J. Schwartz, and D. Burgess, Observations of suprathermal ions in asso-
308 ciation with SLAMS, *Geophys. Res. Lett.*, 20, 149–152, 1993.
- 309 Gurnett, D. A., and A. Bhattacharjee, *Introduction to Plasma Physics*, Cambridge Uni-
310 versity Press, 2005.
- 311 Hellinger, P., and A. Mangeney, Electromagnetic ion beam instabilities: Oblique pulsa-
312 tions, *J. Geophys. Res.*, 104, 4669–4680, 1999.
- 313 Hoppe, M., and C. Russell, On the nature of ULF waves upstream of planetary bow
314 shocks, *Advances in Space Research*, 1(1), 327 – 332, 1981.
- 315 Hoppe, M. M., and C. T. Russell, Plasma rest frame frequencies and polarizations of
316 the low-frequency upstream waves - ISEE 1 and 2 observations, *J. Geophys. Res.*, 88,
317 2021–2027, 1983.

- 318 Khrabrov, A. V., and B. U. Ö. Sonnerup, Magnetic variance analysis for small-amplitude
319 waves and flux transfer events on a current sheet, *J. Geophys. Res.*, *103*, 11,907–11,918,
320 1998.
- 321 Lucek, E. A., T. S. Horbury, A. Balogh, I. Dandouras, and H. Rème, Cluster observations
322 of Hot Flow Anomalies, *Journal of Geophysical Research (Space Physics)*, *109*(A18),
323 A06,207, 2004.
- 324 Lucek, E. A., T. S. Horbury, I. Dandouras, and H. Rème, Cluster observations of the
325 Earth's quasi-parallel bow shock, *Journal of Geophysical Research (Space Physics)*,
326 *113*(A12), A07S02, 2008.
- 327 Mann, G., H. Luehr, and W. Baumjohann, Statistical analysis of short large-amplitude
328 magnetic field structures in the vicinity of the quasi-parallel bow shock, *J. Geophys.*
329 *Res.*, *99*, 13,315, 1994.
- 330 Martinecz, C., et al., Location of the bow shock and ion composition boundaries at Venus
331 Initial determinations from Venus Express ASPERA-4, *Planetary and Space Science*,
332 *56*(6), 780 – 784, 2008.
- 333 Mazelle, C., et al., Production of gyrating ions from nonlinear wave-particle interaction
334 upstream from the Earth's bow shock: A case study from Cluster-CIS, *Planet. Space.*
335 *Sci.*, *51*, 785–795, 2003.
- 336 Meziane, K., et al., Bow shock specularly reflected ions in the presence of low-frequency
337 electromagnetic waves: a case study, *Annales Geophysicae*, *22*, 2325–2335, 2004.
- 338 Ness, N. F., K. W. Behannon, R. P. Lepping, Y. C. Whang, and K. H. Schatten, Magnetic
339 Field Observations near Venus: Preliminary Results from Mariner 10, *Science*, *183*,
340 1301–1306, 1974.

- 341 Omid, N., and D. Winske, Steepening of kinetic magnetosonic waves into shocklets -
342 Simulations and consequences for planetary shocks and comets, *J. Geophys. Res.*, *95*,
343 2281–2300, 1990.
- 344 Pérez-de-Tejada, H., R. Lundin, S. Barabash, J. Sauvaud, A. Coates, T. L. Zhang, D. Win-
345 ningham, M. Reyes-Ruiz, and H. Durand-Manterola, Plasma transition at the flanks
346 of the Venus ionosheath: Evidence from the Venus Express data, *J. Geophys. Res.*,
347 *116*(A15), A01103, 2011.
- 348 Russell, C. T., R. C. Elphic, and J. A. Slavin, Initial Pioneer Venus magnetic field results
349 - Dayside observations, *Science*, *203*, 745–748, 1979.
- 350 Russell, C. T., E. Chou, J. G. Luhmann, P. Gazis, L. H. Brace, and W. R. Hoegy, Solar
351 and interplanetary control of the location of the Venus bow shock, *J. Geophys. Res.*,
352 *93*, 5461–5469, 1988.
- 353 Scarf, F. L., R. W. Fredricks, L. A. Frank, C. T. Russell, P. J. Coleman, Jr., and M. Neuge-
354 bauer, Direct correlations of large-amplitude waves with suprathermal protons in the
355 upstream solar wind., *J. Geophys. Res.*, *75*, 7316–7322, 1970.
- 356 Scholer, M., H. Kucharek, and I. Shinohara, Short large-amplitude magnetic structures
357 and whistler wave precursors in a full-particle quasi-parallel shock simulation, *J. Geo-
358 phys. Res.*, *108*, 1273, 2003.
- 359 Schwartz, S. J., Magnetic field structures and related phenomena at quasi-parallel shocks,
360 *Advances in Space Research*, *11*, 231–240, 1991.
- 361 Schwartz, S. J., and D. Burgess, Quasi-parallel shocks - A patchwork of three-dimensional
362 structures, *Geophys. Res. Lett.*, *18*, 373–376, 1991.

- 363 Schwartz, S. J., D. Burgess, W. P. Wilkinson, R. L. Kessel, M. Dunlop, and H. Luehr,
364 Observations of short large-amplitude magnetic structures at a quasi-parallel shock, *J.*
365 *Geophys. Res.*, *97*, 4209–4227, 1992.
- 366 Sibeck, D. G., et al., Comprehensive study of the magnetospheric response to a hot flow
367 anomaly, *J. Geophys. Res.*, , *104*, 4577–4594, 1999.
- 368 Slavin, J. A., et al., The solar wind interaction with Venus - Pioneer Venus observations
369 of bow shock location and structure, *J. Geophys. Res.*, , *85*, 7625–7641, 1980.
- 370 Smith, E. J., L. Davis, Jr., P. J. Coleman, Jr., and C. P. Sonett, Magnetic Measurements
371 near Venus, *J. Geophys. Res.*, *70*, 1571–1586, 1965.
- 372 Svedhem, H., et al., Venus Express - The first European mission to Venus, *Planetary and*
373 *Space Science*, *55*, 1636–1652, 2007.
- 374 Titov, D. V., et al., Venus Express science planning, *Planet. Space. Sci.*, *54*, 1279–1297,
375 2006.
- 376 Tsubouchi, K., and B. Lembège, Full particle simulations of short large-amplitude mag-
377 netic structures (SLAMS) in quasi-parallel shocks, *Journal of Geophysical Research*
378 *(Space Physics)*, *109*(A18), A02114, 2004.
- 379 Tsurutani, B. T., and P. Rodriguez, Upstream waves and particles: An overview of ISEE
380 results, *J. Geophys. Res.*, *86*, 4319–4324, 1981.
- 381 Tsurutani, B. T., E. J. Smith, and D. E. Jones, Waves observed upstream of interplanetary
382 shocks, *J. Geophys. Res.*, *88*, 5645–5656, 1983.
- 383 Tsurutani, B. T., E. J. Smith, R. M. Thorne, J. T. Gosling, and H. Matsumoto, Steepened
384 magnetosonic waves at Comet Giacobini-Zinner, *J. Geophys. Res.*, *92*, 11,074–11,082,
385 1987.

- 386 Tsurutani, B. T., E. J. Smith, H. Matsumoto, A. L. Brinca, and N. Omidi, Highly non-
387 linear magnetic pulses at Comet Giacobini-Zinner, *Geophys. Res. Lett.*, *17*, 757–760,
388 1990.
- 389 Tsurutani, B. T., J. K. Arballo, E. J. Smith, D. Southwood, and A. Balogh, Large-
390 amplitude magnetic pulses downstream of the Jovian bow shock: Ulysses observations,
391 *Planet. Space. Sci.*, *41*, 851–856, 1993a.
- 392 Tsurutani, B. T., D. J. Southwood, E. J. Smith, and A. Balogh, A survey of low frequency
393 waves at Jupiter: The ULYSSES encounter, *J. Geophys. Res.*, *98*, 21,203, 1993b.
- 394 Wilson, L. B., III, C. A. Cattell, P. J. Kellogg, K. Goetz, K. Kersten, J. C. Kasper,
395 A. Szabo, and K. Meziane, Low-frequency whistler waves and shocklets observed at
396 quasi-perpendicular interplanetary shocks, *J. Geophys. Res.*, *114*(A13), A10106, 2009.
- 397 Zhang, T. L., J. G. Luhmann, and C. T. Russell, The magnetic barrier at Venus, *J.*
398 *Geophys. Res.*, , *96*, 11,145–+, 1991.
- 399 Zhang, T. L., et al., Magnetic field investigation of the Venus plasma environment: Ex-
400 pected new results from Venus Express, *Planet. Space. Sci.*, *54*, 1336–1343, 2006.
- 401 Zhang, T. L., et al., Induced magnetosphere and its outer boundary at Venus, *Journal of*
402 *Geophysical Research (Planets)*, *113*(E12), E00B20, 2008.

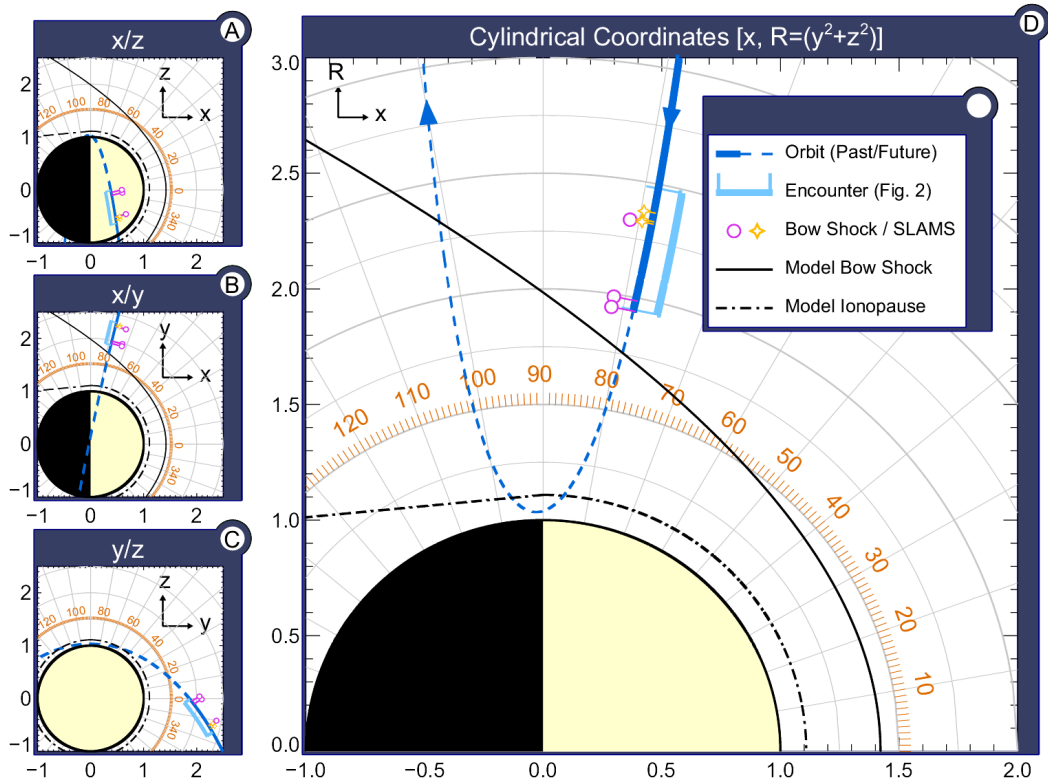


Figure 1. Map of the encounter on the 11th of April 2009, showing the trajectory of *Venus Express* (dark blue line), idealized bow shock according to *Slavin et al.* [1980] (black line), actual bow shock crossings, and the distance covered by the spacecraft during the period covered by Figure 2. Panels A-C are in VSO co-ordinates, Panel D in Cylindrical co-ordinates, where the x-axis points towards the sun, and the y-axis is the radial distance ($R = \sqrt{y^2 + z^2}$) from the Venus/Sun line. All units are in Venus Radii.

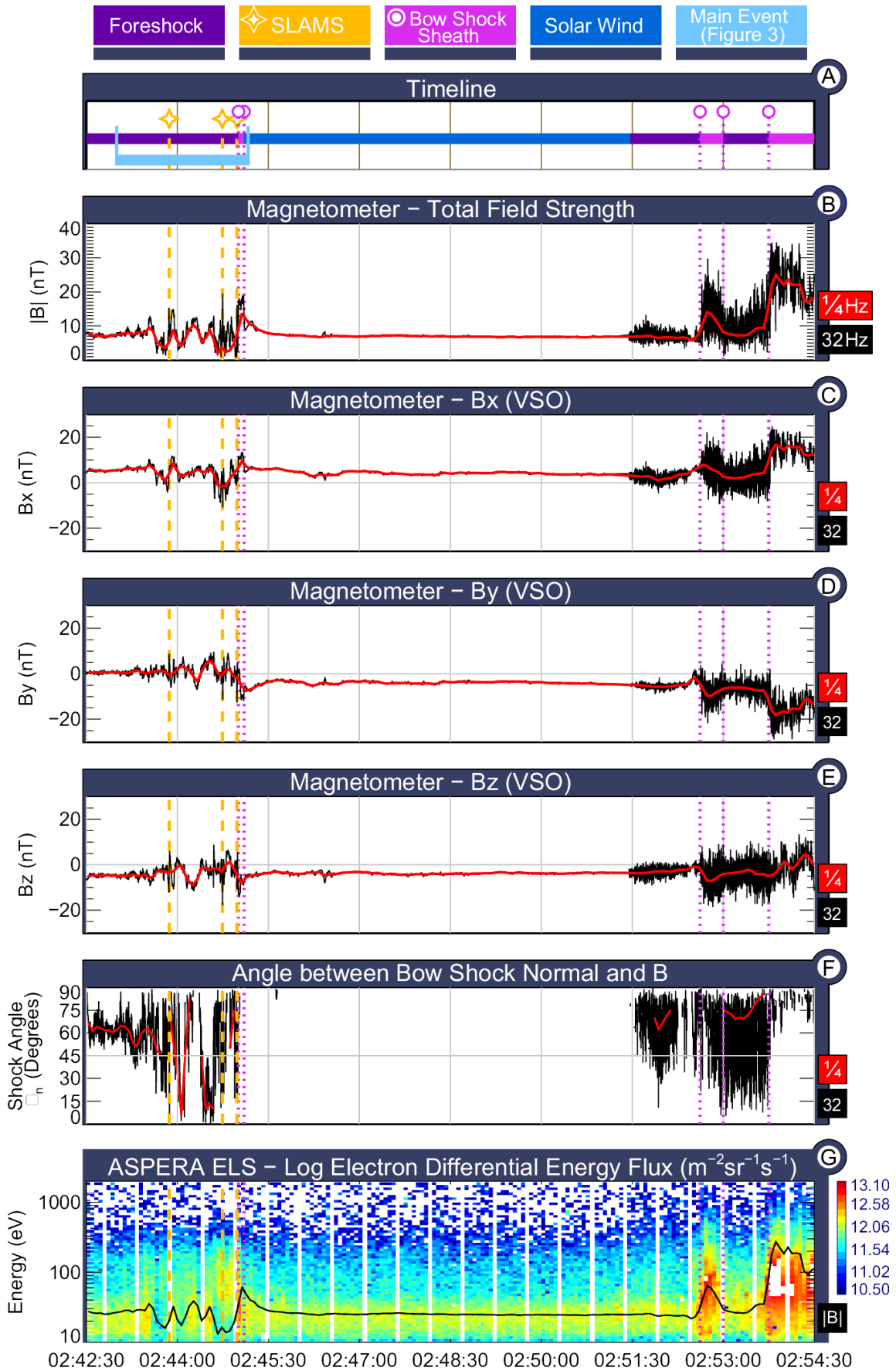


Figure 2. Data from the *Venus Express* on the 11th of April 2009 covering a period from 2:42:30 to 2:54:30 Greenwich Mean Time.
 D R A F T August 27, 2012, 1:05pm D R A F T

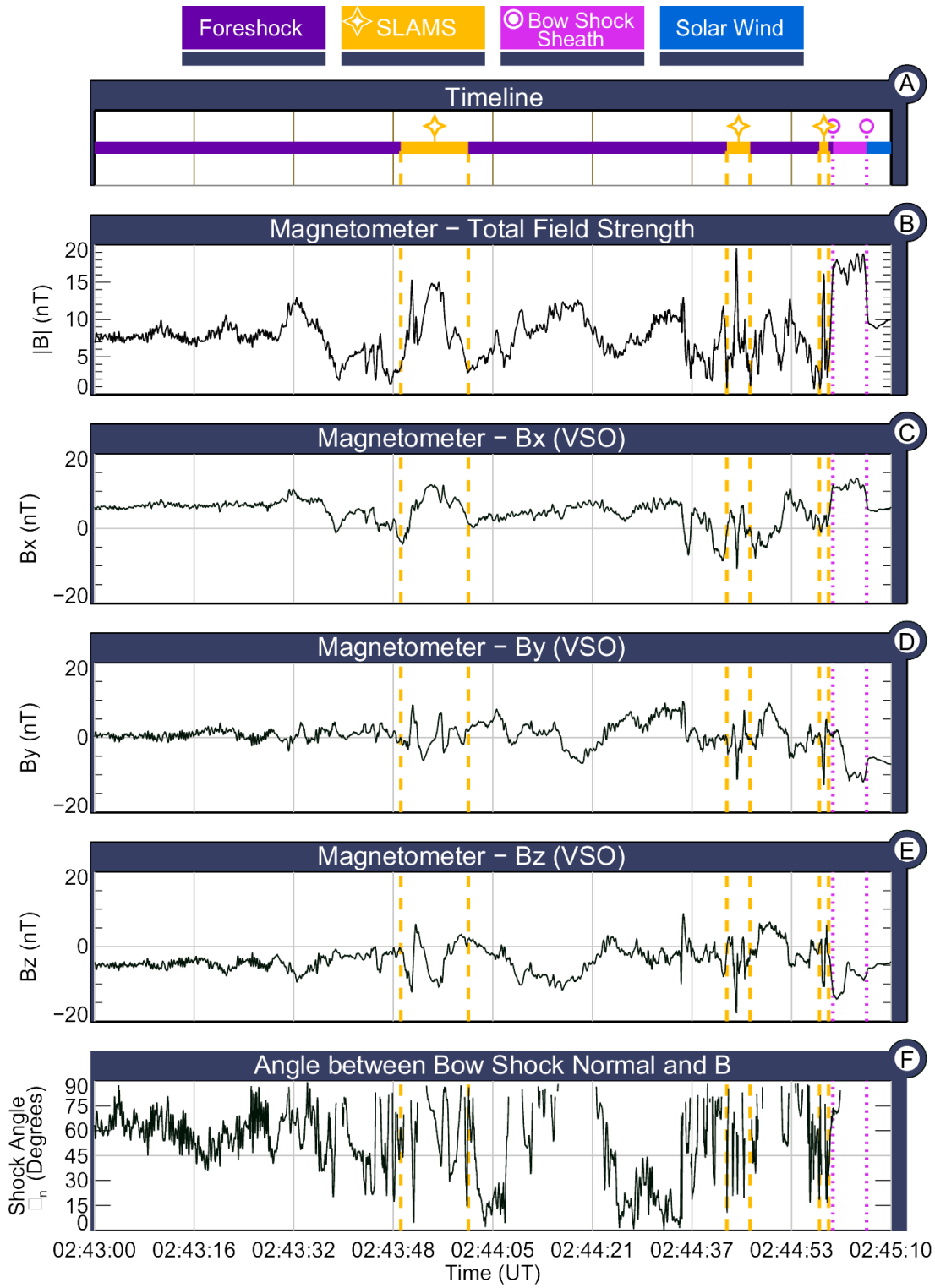


Figure 3. Data from the *Venus Express* on the 11th of April 2009 covering a period from 2:43:00 to 2:45:10 GMT.

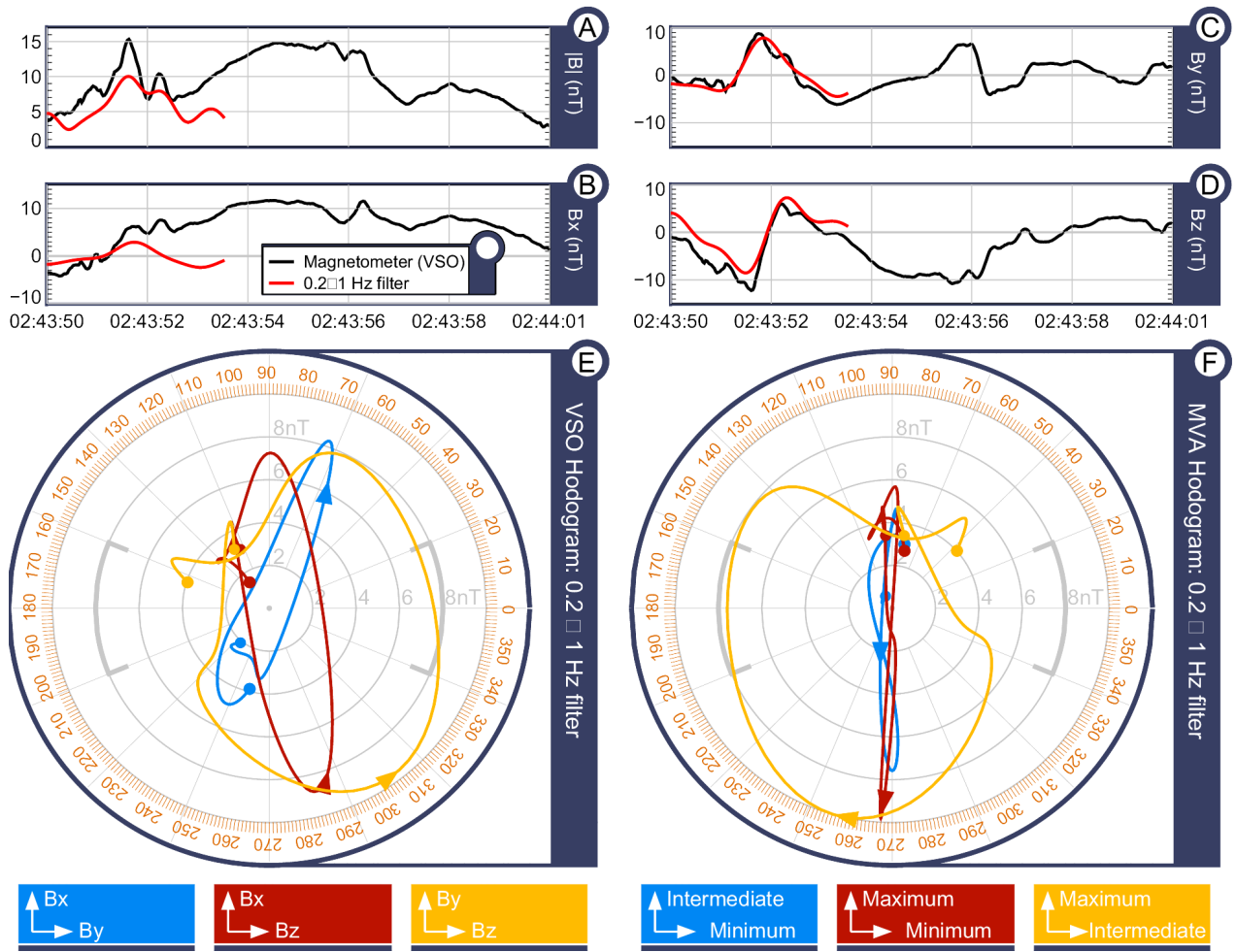


Figure 4. Panels A-D: The magnetic signature of the elliptically polarized field spike within an example of Cytherean SLAMS, at $\sim 02:43:51$ GMT. Panel E: Hodograms of the same data after it has been processed with a $0.2 \rightarrow 1\text{ Hz}$ filter. Panel F: Hodogram of the same data in minimum variance coordinates showing the elliptical polarization of the SLAMS and full 360° rotation.